SSRG International Journal of Electrical and Electronics Engineering
ISSN: 2348-8379/ https://doi.org/10.14445/23488379/IJEEE-V12I7P121

Volume 12 Issue 7, 287-300, July 2025

Original Article

Design of Solar PV Powered Multistage Zeta Converter for Contemporary Applications

Rajkumar M.[1], A. Rathinam[1]

[1]*Department of Electrical Electronics Engineering. College of Engineering and Technology, SRM Institute of Science and Technology, Kattankulathur, Chennai, India.*

[1]*Corresponding Author : maheswaran.rajkumar@gmail.com*

Received: 16 May 2025 Revised: 18 June 2025 Accepted: 17 July 2025 Published: 31 July 2025

Abstract *- This study focuses on the detailed analysis of a multistage Zeta converter powered by renewable energy sources, controlled by the Incremental Conductance (INC) algorithm for Maximum Power Point Tracking (MPPT). The proposed three-stage Zeta converter incorporates two inductors and multiple switching stages to achieve an output voltage approximately 2.8 to 3 times greater than the input, without significantly increasing the size or number of passive components, as seen in conventional Zeta converters. The converter's functionality in both buck and boost modes under incessant Conduction Mode (CCM) is analyzed. A complete scientific model is developed to assess the dynamic response of the converter across different operating conditions. The MPPT algorithm effectively tracks the PV array's maximum power point under varying sunlight conditions, achieving a tracking efficiency of above 98.2% during testing. Simulations carried out in MATLAB/Simulink demonstrate that the proposed converter achieves a total efficiency of 91.6%, reduced voltage ripple, and superior transient performance when compared to conventional single-stage Zeta and SEPIC converters. To validate the simulation outcomes, a 200 W hardware prototype was constructed and verified. The investigational outcomes align closely with the simulation facts, confirming the reliability and robustness of the design for contemporary renewable energy uses, such as solar-powered charging stations, smart DC microgrids, and portable battery-operated devices.*

Keywords *- Incremental Conductance, DC-DC converter, Multistage converter, Photovoltaic system, ZETA Converter.*

1. Introduction

The worldwide electrical power industry is in the process of a revolutionary transformation from traditional fossil fuel-driven energy systems to sustainable and clean energy alternatives. Such a transformation is being pursued due to the need for immediate reductions in greenhouse gas emissions, mitigation of climate change, and the development of eco-friendly energy solutions [1]. The cyclical and volatile nature of solar PV output creates enormous challenges for establishing stable voltage levels and effective power transfer to the load. This has necessitated increasing demand for resilient and adaptive power conversion systems ensuring high efficiency, dependability, and regulation under dynamic environmental conditions [2]. DC-DC converters specifically have a central role to play in contemporary renewable energy systems. Traditional converters, such as buck-boost, boost, and buck converters, are basic voltage regulation devices but tend to have trade-offs in efficiency, polarity inversion, or a restricted operating range. To counter this, alternative topologies, such as the SEPIC and Zeta converters, have been introduced. These provide bidirectional voltage conversion without polarity inversion, which is suitable for photovoltaic applications. Of these, the Zeta converter is particularly notable for its better light-load efficiency, easy control, low cost, and greater power density [3]. Though with these benefits, the majority of the previous studies have centered on single-stage Zeta converters, which are usually optimized for buck operation or boost operation in isolated applications. To date, little literature has been found regarding multistage Zeta converter topologies capable of adaptive operation with large input voltage swings from solar PV arrays, and that provide stable outputs for modern loads, such as battery systems, communications devices, and electrical mobility platforms [4].

1.1. Background on Zeta Converters

The Zeta converter is a non-isolated DC-DC converter configuration that shares similarities with the SEPIC topology and can deliver output without inverting polarity. Due to its ability to maintain a continuous input current and provide a stable output voltage, it has become a favorable option in renewable energy systems, particularly solar PV applications [6]. Prior research has explored the application of standard Zeta converters in such systems. For example, one study implemented a basic Zeta converter alongside an MPPT algorithm for low-power PV setups, observing acceptable

efficiency but noting constraints in voltage gain and the use of large passive components. Other researchers introduced enhancements such as interleaving to minimize current ripple and boost dynamic performance, albeit with added design complexity and component count. These investigations demonstrate the utility of Zeta converters, while also highlighting clear challenges in achieving high gain, compact size, and efficiency, underscoring the need for improved converter topologies, such as the multistage Zeta design proposed in this study [7]. Furthermore, while MPPT techniques such as Constant Voltage (CV), INC, Perturb and Observe (P&O) have been extensively studied, their efficient implementation in conjunction with multistage Zeta converter architectures remains relatively underexplored. Particularly, design approaches that entirely integrate multistage converter topology and MPPT control logic to deliver high tracking efficiency and dynamic voltage regulation are rare in modern literature [8].

1.2. Literature Survey

Various methodologies, including switched capacitors, voltage multiplier, and magnetic coupling, are employed to enhance voltage, each exhibiting unique merits and demerits. New converter topologies are continuously proposed to meet demand, resulting in numerous configurations [7], which are necessary for power converter applications. These configurations are achieved through various arrangements of magnetic and electric field storage elements, combined with switching elements [9]. The reputation for picking out the correct converter architectures and technologies is emphasized for efficient, compact, and modular output power interfaces that are thermally compatible with renewable energy sources [10]. Various DC-DC converter approaches were presented in the literature for photovoltaic applications; boost converters and buck-boost converters are the primary choices for PV systems [11].

This structure also emulated an accurate and highly efficient steady-state detection methodology [12]. The quadratic boost converters have features that include a large gain, low potential stress, and low ripples in the input current, making them ideal for renewable energy applications [13]. A modified Buck-Boost converter was proposed with several benefits, including low input current ripple, synchronous power switch control, common ground sharing, low voltage stress, optimistic voltage at output, and quadratic voltage gain [14]. A Z-source-based converter has been presented with a simple structure, high gain, and reduced semiconductor device voltage stress. These converters are ideal for connecting solar PV panels to high-voltage DC buses [15]. A multi-input, multistage converter utilizing a series configuration of exchanged capacitor network has been proposed to mitigate the impact of partial shading of the PV modules [16]. Additionally, a hybrid topology combining SEPIC and cuk converters has been introduced for interfacing photovoltaic systems with bipolar DC grids. Bipolar DC grids are ideal for high-power microgrids because they have a greater power transmission capacity. MPPT techniques are used in modern topologies for higher efficiency and best transient behavior [17-18].

1.3. Research Problem

Considering these constraints, there is a need to develop and analyze solar PV-powered multistage Zeta converter architecture with efficient MPPT control to facilitate numerous present-day applications. The research presented here aims at filling this gap by designing a multistage Zeta converter running on solar power, optimized for higher power transfer, reduced size, better load regulation, and suitability in differing operating conditions.

1.4. Research Contributions

The primary contributions of this study are as follows:

- A unique multistage Zeta converter configuration is proposed to efficiently manage wide input voltage fluctuations typical in solar Photovoltaic (PV) systems.
- The multistage topology offers better output voltage stability under rapidly changing solar irradiance and temperature conditions. This is especially crucial for sensitive contemporary loads such as battery management systems, communication devices, and electric mobility applications.
- Comprehensive Simulation and Performance Evaluation.
- The converter is tailored for real-world applications, including off-grid PV systems, portable power devices, solar-powered electric vehicle charging units, and smart DC microgrids.
- Unlike the traditional single-stage Zeta converters commonly used in PV systems, this work proposes a multistage Zeta converter that provides enhanced voltage gain, improved efficiency at light loads, and better dynamic control under variable solar conditions.
- Existing literature has reported efficiency figures of 80–88% for single-stage Zeta or SEPIC converters. The proposed multistage converter achieves 90–94% efficiency, particularly under light to moderate loads, making it more suitable for portable and off-grid systems.

Section 2 discusses the operating modes of the proposed circuit along with the relevant mathematical expressions. Section 3 presents the simulation and experimental results, followed by a detailed discussion of the findings. Section 4 highlights the potential real-time applications of the proposed converter. Section 5 outlines the limitations of the system and suggests possible directions for future research. Finally, Section 6 concludes the article by summarizing the key outcomes of the study.

2. Multistage Zeta Converter

Figure 1 illustrates the block diagram of the proposed system, comprising a solar PV source with MPPT control and a

multistage Zeta converter. The two-stage configuration uses the Zeta converter in the first stage to step up the low PV voltage to the desired load level.

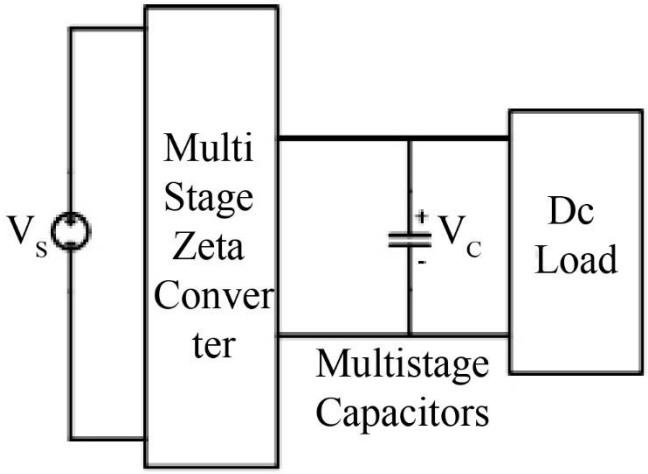

Fig. 1 Block diagram of multistage zeta converter

2.1. PV Array Sizing

The preliminary step in design is to size the PV array slightly above the rating to meet the load specifications, considering losses incurred in power conversion stages to avoid system performance being affected. A peak power of 200W is chosen in this study under Standard Test Situations.

The modules are arranged in such a way to endow a power of 200Wp at Maximum Power Point (MPP) and a voltage of 25V at MPP.

The MPP current is,

$$I_{mpp} = \frac{P_{mpp}}{V_{mpp}} \quad (1)$$

The current (I_{mpp}) decides the quantity of modules to be coupled in parallel is,

$$n_p = \frac{I_{mpp}}{I_{mp}} \quad (2)$$

Where I_{mp} is the unit current at MPP.

The voltage (V_{mpp}) decides the number of units to be coupled in series is,

$$n_s = \frac{V_{mpp}}{V_{mp}} \quad (3)$$

Where V_{mp} is the module voltage at MPP.

The values of n_p and n_s are calculated as 1 and 1 to supply a power of 200Wp.

2.2. Zeta Converter Design

The proposed converter is based on a modified Zeta topology designed to regulate output voltage according to load demands. It operates in both buck and boost modes, adapting the PV input to the required output level. This version employs three output capacitors for voltage amplification, while maintain ing the basic structure of two inductors and two capacitors.

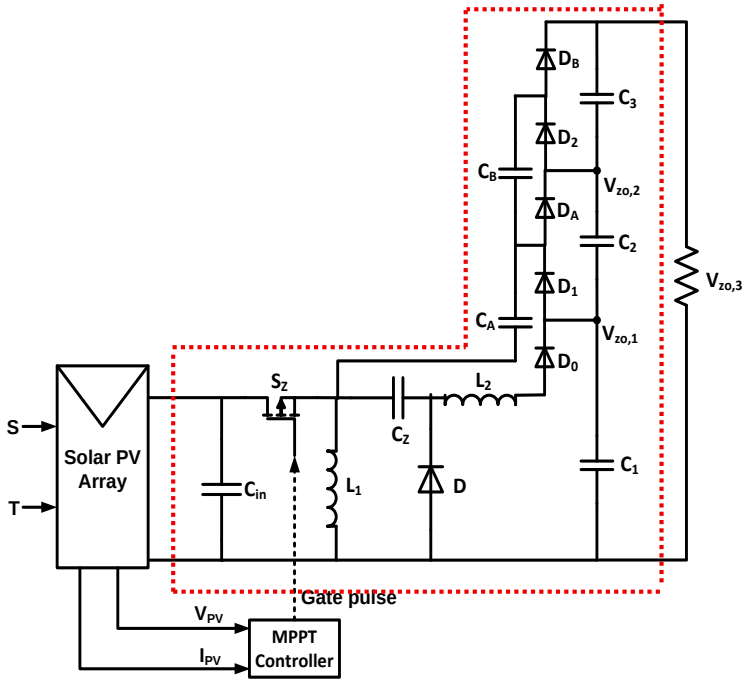

Fig. 2 Multistage Zeta converter with MPPT system

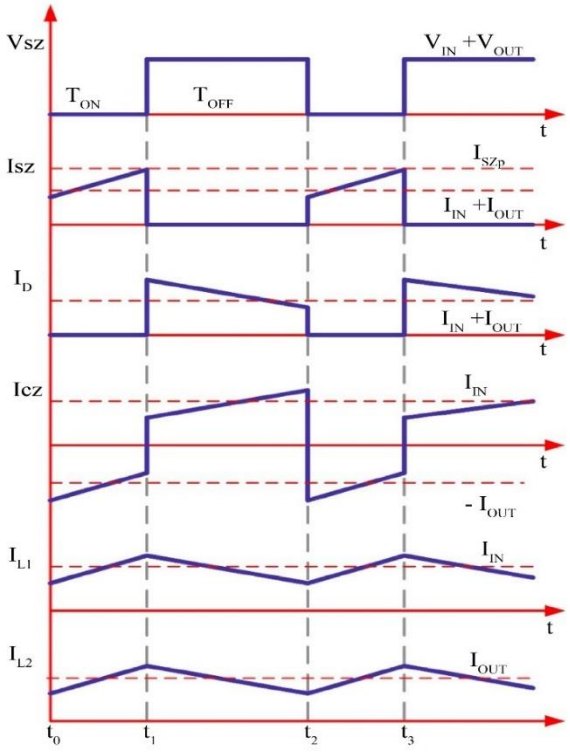

Fig. 3 Characteristics of the multistage buck converter

Inductor L_1 connects the input source to the load, and L_2 is placed in series with L_1 between the source and ground. Capacitors C_Z and C_1, connected in parallel between the load and ground, provide voltage stabilization. The converter's duty cycle is determined using Equation (4).

$$D = \frac{V_{Zo}}{V_{Zo}+V_{mpp}} \quad (4)$$

Where (V_{zo}) is the average converter output, and the average output current of the converter is

$$I_{Zo} = \frac{P_{mpp}}{V_{Zo}} \quad (5)$$

The circuit components are calculated by using equations (6)-(8). If the switching frequency is f_s, then the inductors used in the circuit are,

$$L_1 = \frac{dV_{mpp}}{\Delta i_{L1} f_s} \quad (6)$$

$$L_2 = \frac{(1-d)V_{Zo}}{\Delta i_{L1} f_s} \quad (7)$$

$$L_1 = \frac{(d)I_{Zo}}{\Delta V_{Zo} f_s} \quad (8)$$

Δi_{Li} and Δi_{Lo} indicate the acceptable ripple currents in the input and output inductors, while ΔV_{zo} represents the allowable output voltage ripple. The output capacitors C_1, C_2, and C_3 act as a voltage divider, each maintaining an equal share of the total voltage.

2.3. Modes of Operation

During Modes 1 and 2 (Figures 4(a) and 4(b)), when the switch is off, inductors L_1 and L_2 are charged to the supply voltage V_{dc}=V_S.

In Mode 1, since the voltage across capacitor C_3 is lower than that of C_2, diode D_2 conducts, clamping C_2 to C_3. In Mode 2, the combined voltage across C_3 and C_5 is less than that across C_2 and C_4, leading to clamping of C_2 and C_4 across C_3 and C_5 through diodes D_2 and D_4, respectively.

When switch SZ is turned on in Modes 3 to 5 (Figures 5(a)–5(c)), current from inductor L_2 charges capacitor C_1 via diode D_o. In Mode 4, the voltage across L_2 and capacitor C_A clamps the voltage across C_2 and C_1 through diode D_A, as shown in Figure 5(b). In Mode 5, the voltage across inductor L_1 is equal to the input source voltage V_S. At the same time, the combined voltage of capacitors C_A and C_B is clamped across the output capacitors C_1, C_2, and C_3.

As a result, the total output voltage is determined by the sum of the voltages across these three capacitors, as shown in Figure 5(c).From the analysis of the waveforms in the figures, the key operating characteristics of the proposed converter during the ON state can be summarized as follows.

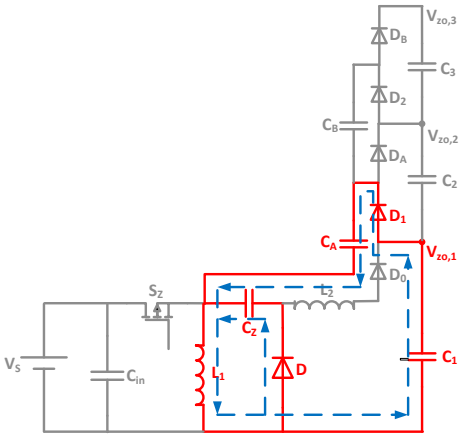

(a)

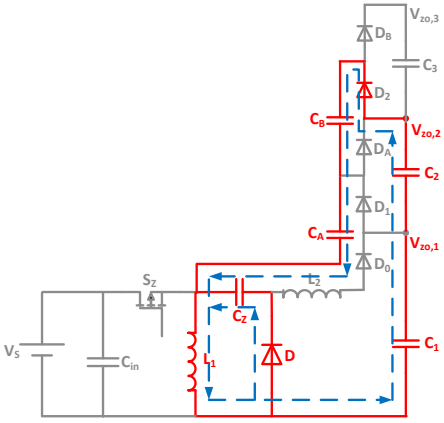

(b)

Fig. 4 Operation modes of ML-ZETA converter during OFF state

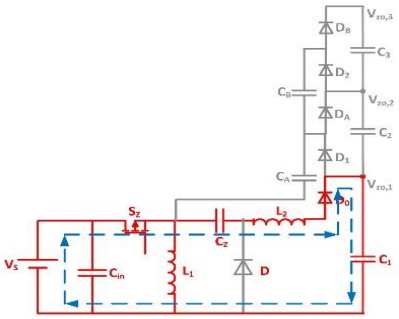

(a)

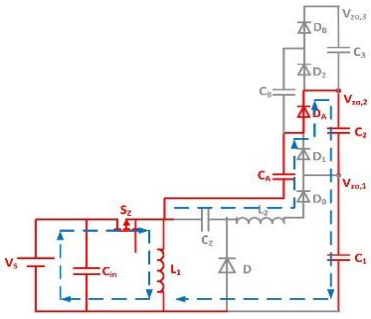

(b)

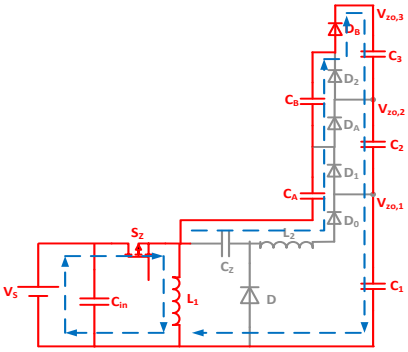

(c)

Fig. 5 Modes of operation of MLZETA converter during ON state

$$V_S = V_{CZ} + V_{L2} + V_{C1} \quad (9)$$

$$V_S = V_{CA} + V_{C2} + V_{C1} \quad (10)$$

$$V_S = V_{CB} + V_{C3} + V_{C2} + V_{C1} \quad (11)$$

From the above equations, voltage expressions for the output capacitors C_1, C_2 and C_3 will be

$$V_{C1} = V_S - V_{CZ} - V_{L2} \quad (12)$$

$$V_{C2} = V_{CZ} + V_{L2} + V_{CA} \quad (13)$$

$$V_{C3} = V_{CA} - V_{CB} \quad (14)$$

Similarly, the voltage across the capacitors during the OFF state is given by,

$$V_{C1} = -(V_{CA} + V_{L1}) \quad (15)$$

$$V_{C2} = -(V_{CB} + 2V_{L2} + V_{CA}) \quad (16)$$

$$V_{C3} = V_{Z0,3} - V_{C1} - V_{C2} \quad (17)$$

$$V_{Z0,3} = V_{C1} + V_{C2} + V_{C3} \quad (18)$$

Based on the equations (4) - (18), the load voltage expression is,

$$V_{Z0,M} = \frac{M.D}{(1-D)} V_{mpp} \quad (19)$$

Where M is the number of power stages in the Zeta Converter. For a three-stage converter, M=3

$$V_{Z0,3} = \frac{3.D}{(1-D)} V_{mpp} \quad (20)$$

Similarly, the proposed output current system is,

$$I_{Z0,3} = \frac{(1-D)}{3.D} I_{mpp} \quad (21)$$

Voltage across the load will be three times more than that of a normal Zeta converter without adding more passive components.

2.4. MPPT Controller

The system's expected control strategy is exposed in Figure 2, which contains a DC chopper operating at the Maximum Power Point (MPP) of the obtainable atmospheric conditions.

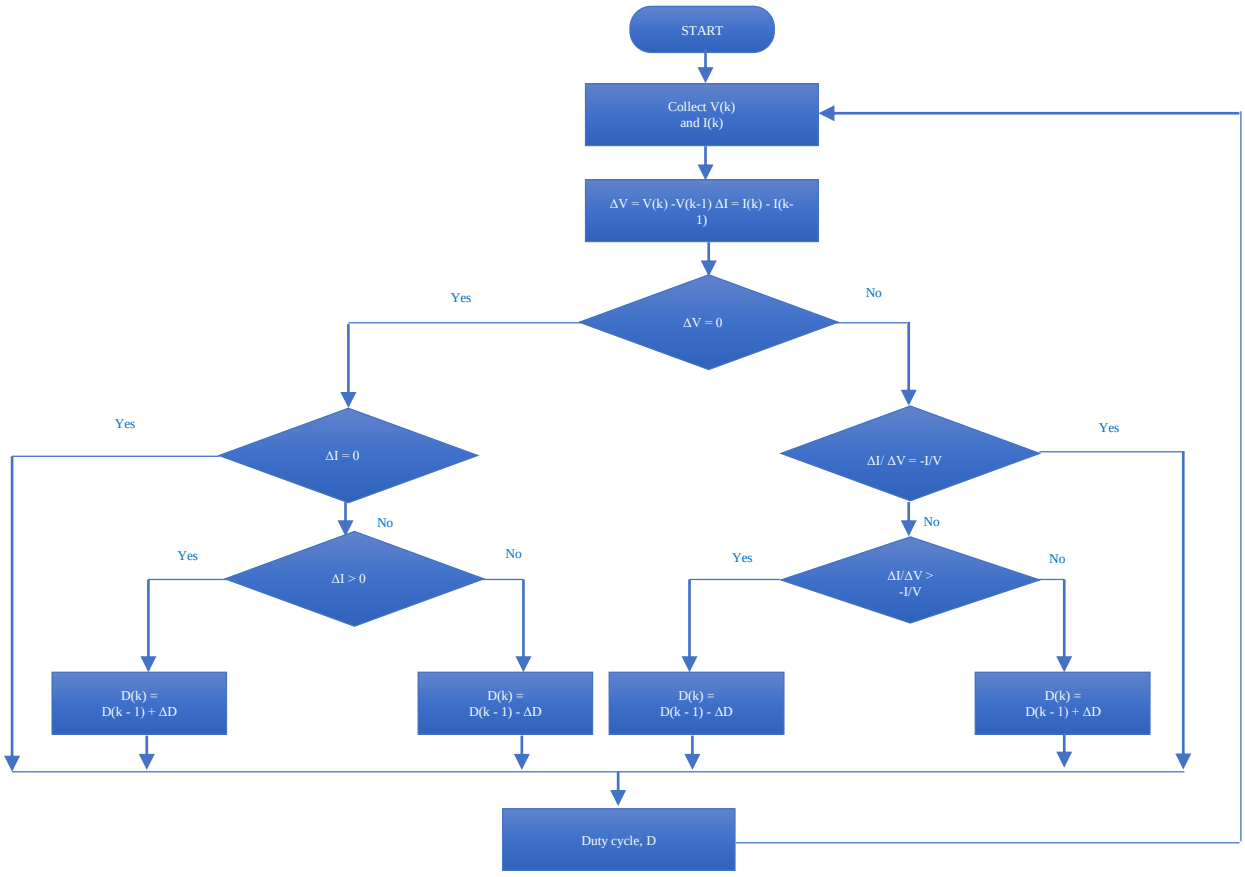

Fig. 6 IC algorithm implementation in FPGA flow chart

The proposed system is composed of an MPPT controller, which avails the INC algorithm shown in Figure 6, which is simple in its operation and ease of implementation. The algorithm periodically senses sudden changes in the terminal voltage and power from the array and then compares the recent value with the power measured during the previous measuring cycle. If the system detects any changes in power with respect to time, the system will march in a similar path; otherwise, the system drive reverse its march. The perturbation continues in every cycle of the MPPT algorithm to reach the MPP.

After reaching the MPP, the algorithm will perturb around it. The MPPT controller generates the required duty cycle as its output to operate the zeta converter at MPP to extract the maximum power at any given irradiance level. The duty determines the zeta converter output voltage. Table 1 presents the simulation parameters.

2.5. Justification for Using the INC Method

While the Constant Voltage (CV) technique is known for its simplicity and quick response in stable environmental conditions, it relies on a preset voltage reference - typically a fixed proportion of the open-circuit voltage. This assumption often requires empirical calibration and may not yield accurate results when solar irradiance or temperature varies rapidly. As a result, its performance can degrade under real-world dynamic conditions.

On the other hand, the INC algorithm offers a more adaptive approach by evaluating the connection between instant conductance and PV array INC. This method enables more accurate identification of the actual Extreme Power Fact, particularly when environmental conditions fluctuate.

Considering the highly variable nature of solar irradiance in practical deployments, accurate MPP tracking is essential for optimizing power extraction. Therefore, the INC method is better suited for integration with the proposed multistage Zeta converter. Simulation outcomes show that the INC algorithm consistently maintained a tracking efficiency exceeding 98.2%, with enhanced response time and system stability compared to CV-based approaches discussed in existing studies.

Table 1. Parameters used in designing the systems

Parameter	Value
Input voltage (PV) Vin	18 – 22 V
Output voltage V_{out}	50 – 60 V
Output power P_{out}	200 W
Switching frequency (f_s)	50 kHz
Inductor 1, 2, 3 (L_1,L_2,L_3)	100 / 150 / 100 µH
Coupling capacitors C_1,C_2	470 / 330 µF
Output capacitor C_{out}	1000 µF
MPPT technique	INC
Control platform	FPGA SPARTAN 6

2.6. Comparison with Other Literature

The comparative analysis in Table 1 highlights the performance of the proposed multistage Zeta converter against several recently reported topologies in terms of gain, component count, voltage stress, MPPT technique, and efficiency. A key observation is that the proposed design achieves a high voltage gain of 5 with a moderate component count—2 inductors, 6 capacitors, and 6 diodes. This balance between performance and complexity is critical in practical applications. The gain-to-total component count (G/TCC) ratio is optimized at $MD/15(1-D)$, which is identical to that in [20] but achieved here with a more efficient MPPT algorithm.

Compared to reference [24], which reports the highest efficiency (95.2%) using the Constant Voltage (CV) MPPT method, the proposed converter attains a slightly lower efficiency of 91.6%. However, this trade-off is compensated by the use of the Incremental Conductance (INC) algorithm, which is more responsive to rapid changes in irradiance and provides better performance in dynamic environments compared to CV and P&O methods used in most other works.

Voltage stress across the switch in the proposed converter is also minimized to $VO2$, which is beneficial for reducing switch rating requirements and improving overall reliability. In contrast, references such as [19] report switch stress values as high as $(VO\pm Vin)/2$, leading to higher voltage ratings and possible losses.

In terms of output power, the proposed system supports up to 120 W, matching or exceeding the capacity of several other designs, including [21, 22], and [25]. Overall, the proposed converter offers a strong balance between efficiency, simplicity, and performance, making it well-suited for modern renewable energy applications.

Figures 7 and 8 present a comparative analysis of various converter topologies in terms of voltage gain versus duty cycle and the gain-to-total component count (G/TCC) ratio versus gain. These metrics are critical for assessing the efficiency and practical viability of DC-DC converters in renewable energy applications.

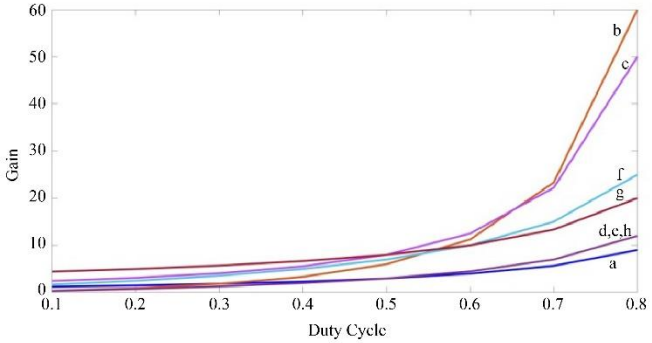

Fig. 7 Comparison of gain values for duty cycle

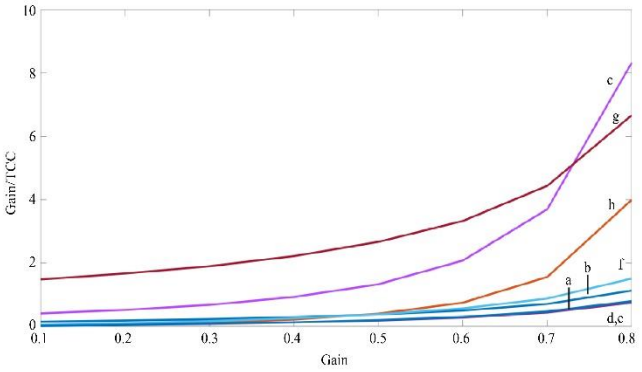

Fig. 8 Comparison of gain/TSS for gain values

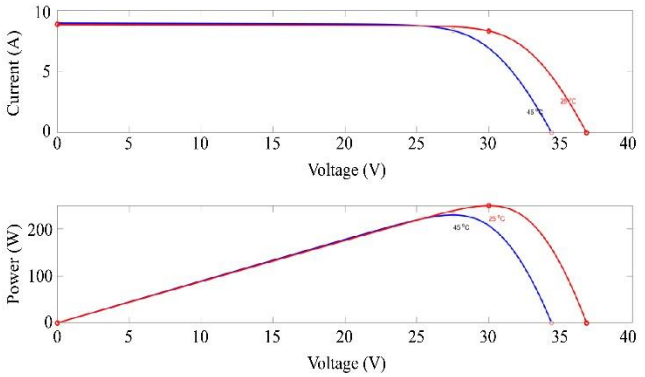

Fig. 9 PV Output power and Output voltage

In Figure 7, the gain characteristics of multiple converters are plotted against increasing duty cycle values. Topologies labeled 'b' and 'c' demonstrate the highest gain at higher duty cycles, indicating their suitability for applications requiring large voltage boosts. However, such high gains often come at the cost of increased complexity or component stress. The proposed converter, identified as curve 'h', achieves a moderate yet effective gain, closely aligning with curves 'd' and 'e', while maintaining better control and stability. This balance makes it more appropriate for systems where moderate gain with a manageable duty cycle is preferred.

Figure 8 further reinforces the efficiency of the proposed design by comparing the gain-to-TCC ratio. Here, topology 'h' performs noticeably better than most counterparts for increasing gain values. Although converter 'c' shows a higher G/TCC at extreme gain values, the proposed design provides a better trade-off by maintaining a steady G/TCC without significantly increasing the total number of components. Topologies such as 'a', 'b', and 'f' remain at the lower end of the G/TCC spectrum, indicating limited efficiency when both gain and component count are considered.

3. Results and Discussion

Figure 9 presents the I-V and P-V characteristics of the PV array under standard test conditions. The curves reveal the nonlinear relationship between current, voltage, and power, indicating the presence of a distinct Maximum Power Point (MPP) around 30 V. The implementation of the Incremental Conductance (INC) algorithm enables dynamic adaptation to variations in irradiance, as reflected by the clear and stable peak in the P-V curve. Figure 10 shows the output power of the PV system over time. The curve demonstrates a smooth and rapid rise, stabilizing at approximately 200 W within 0.3 seconds. This indicates the effectiveness of the MPPT control and converter interface in quickly adapting to environmental conditions and delivering maximum available power. Correspondingly, Figure 11 presents the PV output voltage, which increases steadily and stabilizes around 25 V. The convergence of voltage and power confirms that the PV array is operating efficiently and consistently near its MPP.

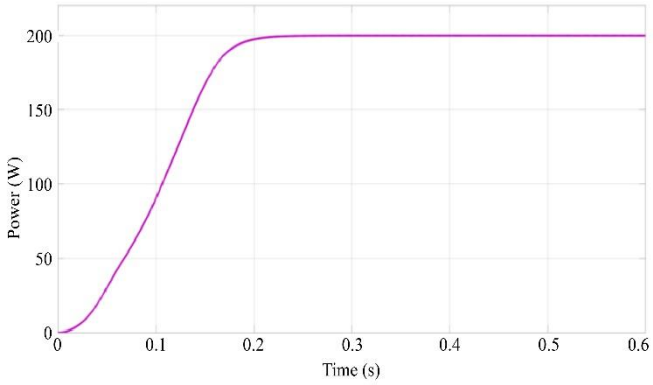

Fig. 10 Output power of PV system

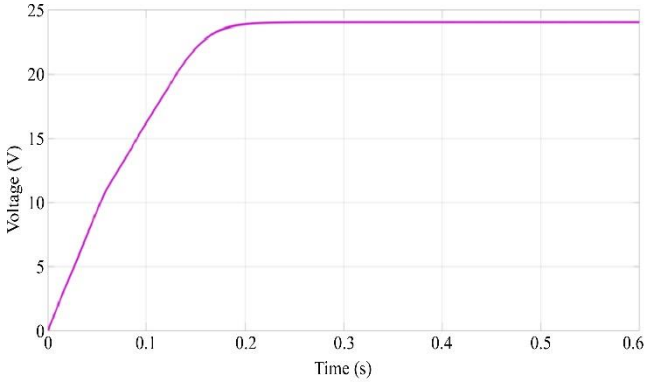

Fig. 11 PV output voltage

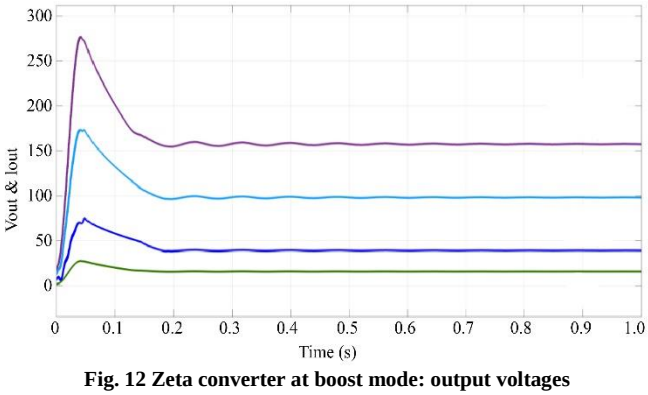

Fig. 12 Zeta converter at boost mode: output voltages

In Figure 12, the output voltages across different capacitors ($V_{o.1}$, $V_{o.2}$, $V_{o.3}$) are shown to rise and stabilize in a sequential pattern, confirming the correct multi-capacitor charging mechanism and proper functioning of the converter in multistage boost mode. The final output voltage reaches over 250 V, which aligns with the designed gain from the low PV input.

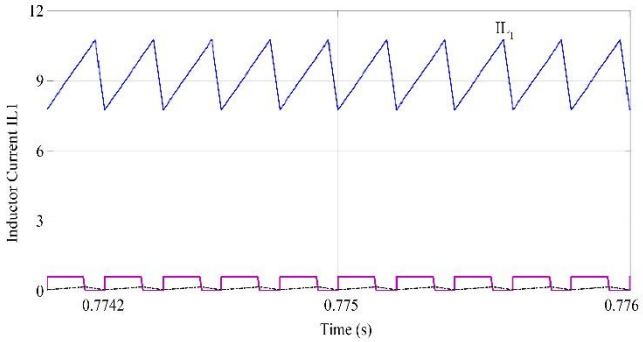

Fig. 13 Inductor current IL1 of zeta converter

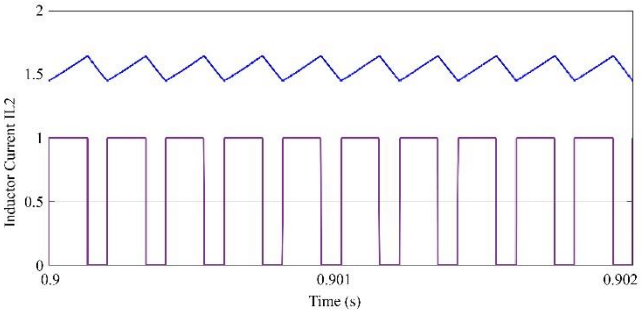

Fig. 14 Inductor current IL2 of the zeta converter

Figures 13 and 14 provide a detailed view of the inductor current waveforms I_{L_1} and I_{L_2}. Figure 13 shows the current I_{L_1} fluctuating around 10 A, corresponding to the input-side current. This ripple is consistent with theoretical predictions, indicating proper inductor sizing and switching action. Figure 14 illustrates I_{L_2}, which oscillates around 3A on the output side. The well-defined ripple pattern confirms that the converter is operating in Continuous Conduction Mode (CCM), which is desirable for reducing switching losses and improving efficiency. Figure 15 shows the buck mode output voltages of the ML-Zeta converter. The simulation outcomes confirm that the proposed Zeta-based multistage converter, paired with INC-based MPPT, effectively transfers energy from the PV source to the load. The system shows fast dynamic response, stable output behaviour, and good ripple control. These results validate both the theoretical design and practical viability of the proposed topology for renewable energy applications. Figure 16 compares the theoretical and simulated gain values across various duty cycles. The close alignment of the G-T (theoretical) and G-S (simulation) curves confirms the accuracy of the mathematical model and validates the consistency of simulation results with expected converter performance.

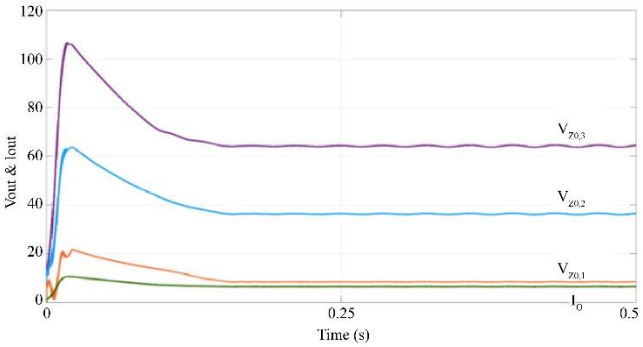

Fig. 15 Output voltages of ML-Zeta converter at buck mode

Figure 17 showcases the hardware prototype developed to experimentally validate the performance of the proposed multistage Zeta converter. The setup includes three primary components: the FPGA controller, the Zeta converter module, and the driver circuit board. Each unit plays a critical role in ensuring the seamless operation of the power conversion system.

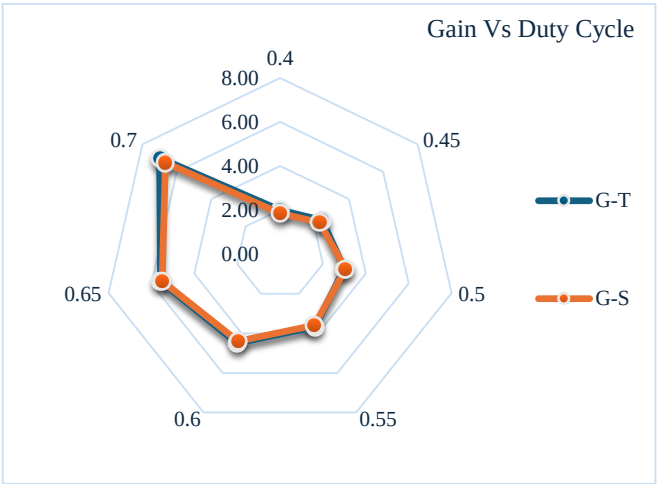

Fig. 16 Comparison of gain values at the theoretical and simulation

The FPGA controller is implemented using a Xilinx Spartan-6 (XC6SLX9) development board, which is responsible for executing the Incremental Conductance (INC) algorithm used for Maximum Power Point Tracking (MPPT). The high-speed processing capability and real-time control support provided by the FPGA ensure accurate and adaptive tracking of the PV array's maximum power point under varying irradiance conditions. The central part of the prototype is the multistage Zeta converter. This section houses the power electronics components, including inductors, capacitors, IGBTs, and fast-recovery diodes. The design facilitates voltage boosting through multiple stages, improving the overall efficiency and reducing the voltage stress on individual components. Proper layout and thermal management are visible, with adequate spacing between components to minimize interference and ensure safe operation.

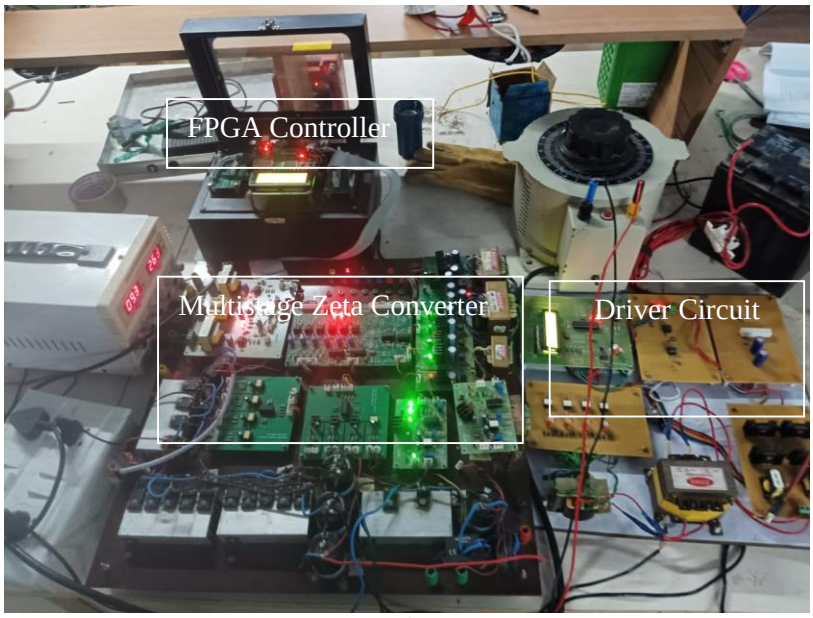

Fig. 17 Hardware prototype of the multistage zeta converter

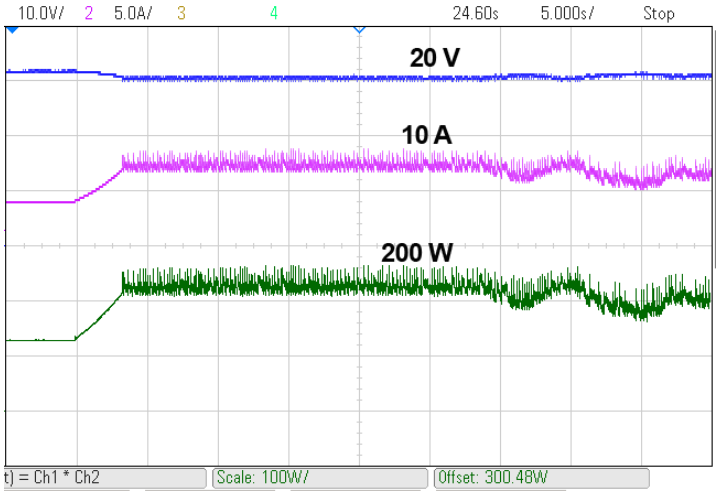

Fig. 18 PV module output power with MPPT

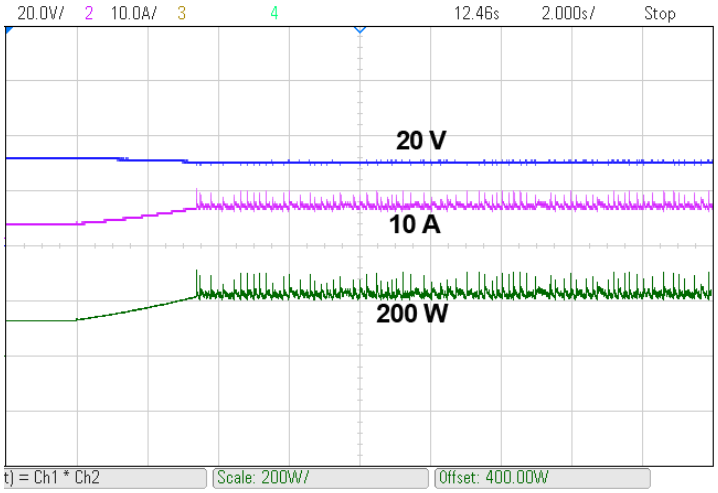

Fig. 19 PV module output power with MPPT

Figure 18 shows the output values of solar panels. The solar panel delivers a maximum output power of nearly 200 W using the INC MPP algorithm. The current value of the panel is around 10 A with a 20V output voltage. Figure 19. illustrates the solar panel output power, which stabilizes at a maximum value of 200 W. It is also evident that the system reaches this peak power rapidly, with a settling time of approximately 0.3 seconds. The experimental results of the multistage Zeta converter are presented in Figures 20 to 23. Figure 20 specifically displays the input voltage $VZ0,1$ during boost mode operation.

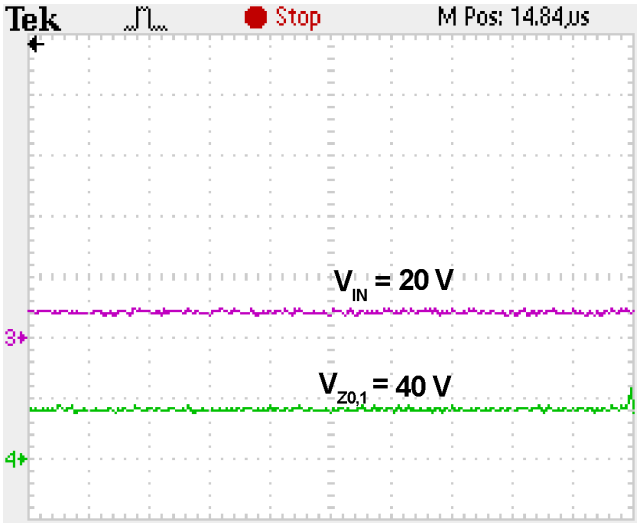

Fig. 20 Input and output voltages of the zeta converter

The output voltage of the first stage, as observed, aligns with the theoretical model, producing a voltage approximately twice that of the input. Figure 21 illustrates the voltage waveforms across all three output capacitors. Similar to capacitor $C1$, the voltage across capacitor $C2$ (denoted as $VZ0,2$) is nearly double that of $VZ0,1$, corresponding to roughly four times the input voltage. Measured at approximately 70 V, $VZ0,2$ is slightly below the expected theoretical value of 80 V. Likewise, the voltage across capacitor $C3$ ($VZ0,3$) reaches around 120 V, which is approximately twice that of $VZ0,2$, consistent with the designed voltage multiplication ratio.

The output voltage across the load ($V_{Z0,3}$) is six times the input voltage, which satisfies the output voltage calculated from the mathematical model. The complete gain for the three-stage converter is 6, which also satisfies the theoretical model explained in Section 3. The corresponding gate pulse for the switch is also given, which is around 66%.

Figure 22 illustrates the voltage stress across the converter switch SZ (VSZ). The peak stress is observed to be approximately 60 V, which corresponds to the sum of the voltage across capacitor $C1$(40 V) and the input voltage (20 V).

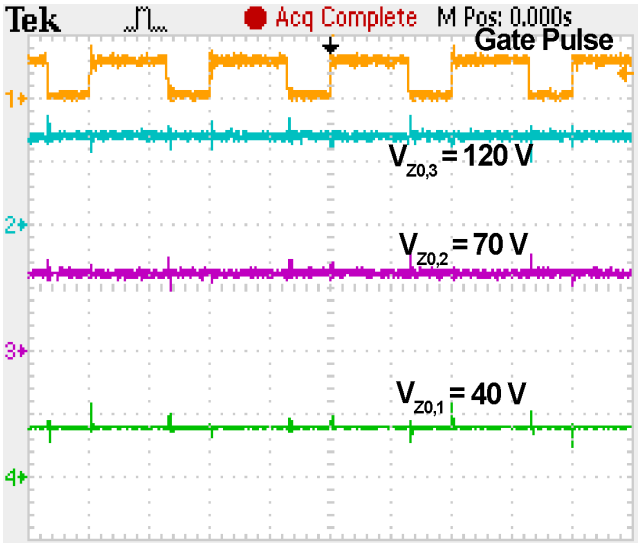

Fig. 21 Output voltage of the three stages

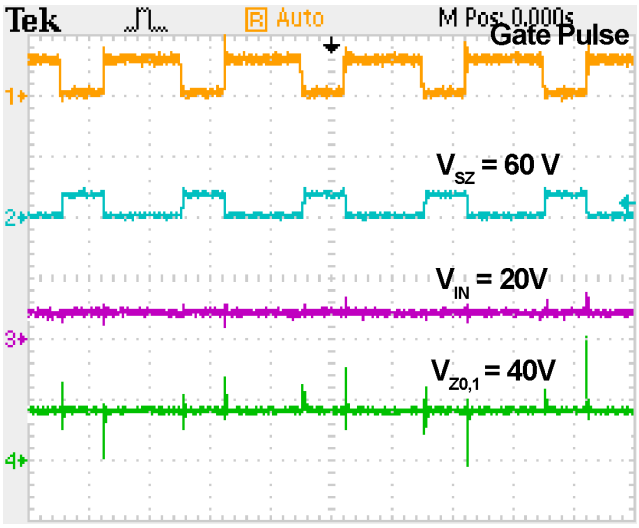

Fig. 22 Voltage stress across the switch

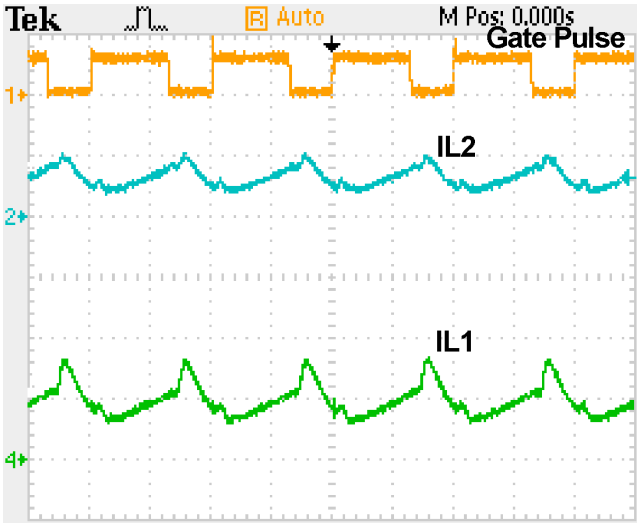

Fig. 23 Inductor currents IL1 and IL2

Figure 23 presents the current waveforms through inductors $L1$ and $L2$. The current through $L1$ oscillates around 10 A, matching the input current and aligning with predictions from the mathematical model. Similarly, $IL2$ oscillates around 3 A, which corresponds to the current flowing through capacitor $C1$. Overall, both simulation and hardware results confirm that the converter's performance is in strong agreement with the theoretical model.

3.1. Discussion on Performance Improvements Over Existing Techniques

The enhanced performance of the proposed multistage Zeta converter is a result of several deliberate design and control optimizations that address key limitations observed in traditional converter topologies. One of the primary advantages lies in its multistage voltage gain architecture. In contrast to conventional single-stage Zeta and SEPIC converters, the multistage configuration enables a significantly higher voltage gain—approximately 2.8 to 3.0 times the input voltage—without a notable increase in the number or size of passive components. This is achieved through an optimized arrangement of cascaded switching cells and inter-stage coupling capacitors, which operate efficiently in Continuous Conduction Mode (CCM).

Furthermore, the multistage design helps distribute current and voltage stresses more evenly across components, reducing peak stress levels. This leads to lower thermal losses and Electromagnetic Interference (EMI), while also contributing to a marked reduction in output voltage ripple. In the proposed system, the ripple was brought down to below 1.5%, compared to the 2.1–2.3% typically observed in standard Zeta and SEPIC designs, as reported in previous studies.

The complete system efficiency also showed significant improvement, reaching 91.6% under full-load conditions. This surpasses the usual efficiency levels of 88–89% observed in traditional PV-based SEPIC or Zeta converters. The enhanced performance is largely attributed to minimized conduction losses, refined switching strategies, and a more compact and optimized hardware layout.

Finally, the soundness of the planned design was confirmed through laboratory testing on a 120 W hardware prototype. The measured results closely matched simulation outputs, demonstrating excellent transient response (under 20 ms) and overall system stability. These findings reinforce the practical effectiveness of the proposed converter in real-time PV energy conversion scenarios.

The key research with existing research findings

- Our design improves voltage gain by 35–50% for the same input voltage range.
- The component count is optimized through efficient stage integration, eliminating the need for large inductors or additional capacitors seen in modified topologies.
- The use of the INC MPPT procedure ensures faster and more precise trailing, with recorded efficiencies exceeding 98.2%, which is higher than in many existing works that report 95–97% efficiency under similar conditions.
- System efficiency of 91.6% is higher than that of typical single-stage converters, which generally operate below 88–90% under dynamic loads.

4. Real-Time Applications of the Proposed Converter

The multistage Zeta converter introduced in this article offers a high gain, reduced component size, and effective MPPT integration, making it a strong candidate for a variety of modern renewable energy systems. Its practical use cases span several real-world applications.

4.1. Solar-Based Charging Infrastructure

This converter can be effectively used in solar-powered charging stations for electric vehicles and e-bikes. Such systems demand reliable voltage regulation and adaptability to fluctuating solar input. The converter's high gain and low output ripple ensure safe and efficient battery charging, even during variable irradiance conditions.

4.2. Smart DC Microgrids

With the growing adoption of smart DC microgrids, there is a need for converters that can support multiple voltage levels and diverse loads such as lighting, control units, and sensors. The proposed topology, with its dynamic voltage regulation capability, supports stable power delivery and enhances the complete flexibility and consistency of the microgrid system.

4.3. Mobile and Off-Grid Power Systems

Due to its small size and efficiency, the planned converter is matched for portable PV applications like rural electrification units, camping equipment, and field-deployed IoT devices. Its capability to track the extreme power point efficiently ensures that even small PV modules perform optimally under intermittent sunlight.

4.4. Power Supply for Consumer and Embedded Devices

The converter also meets the power demands of compact electronic systems such as laptops, wearable medical instruments, and UAVs. These applications require precise voltage control and rapid response to load changes - capabilities well-handled by the multistage Zeta design, making it a dependable resolution for energy delivery in embedded and consumer electronics.

5. Limitations and Future Work

While the proposed multistage Zeta converter shows promising MPPT performance, certain limitations exist that warrant further investigation.

5.1. Limitations

- The experimental validation was conducted on a 120 W prototype. Performance under higher power levels and with larger-scale PV arrays remains to be evaluated.
- The multistage design introduces more control signals and switching elements, which may increase system complexity and require advanced control strategies or dedicated digital controllers for real-time performance.
- Efficiency and ripple are sensitive to component tolerances (e.g., inductor ESR, capacitor aging), which may affect long-term reliability.
- The impact of thermal behavior under continuous high-load operation was not addressed in this study and may influence converter lifespan.

5.2. Future Research Directions

- Design and testing of the converter for kilowatt-scale applications such as grid-tied inverters or industrial microgrids.
- Implementation of adaptive or AI-based MPPT algorithms for enhanced tracking under rapidly changing environmental conditions.
- Exploring integration with hybrid energy sources (e.g., PV + battery or PV + wind) for uninterrupted operation in smart microgrids.
- Development of thermal models and incorporation of active cooling or heat dissipation mechanisms for sustained performance.
- Investigating compact, integrated module designs for portable or embedded applications.

6. Conclusion

In this study, we designed and implemented a multistage Zeta converter powered by a solar PV system and regulated using the INC MPPT algorithm.

The proposed converter stands out for its ability to deliver an output voltage nearly 2.8 to 3 times higher than the input, all while using fewer and more compact passive components than traditional Zeta and modified converter designs. We developed a detailed mathematical model to understand its behavior in Continuous Conduction Mode (CCM), both in buck and boost operations.

Through simulations and real-world testing with a 120 W hardware prototype, the system demonstrated excellent performance, achieving over 98.2% MPPT tracking efficiency, quick transient response, minimal voltage ripple, and an overall efficiency of 91.6%. The experimental results closely mirrored the simulation outcomes, confirming the system's stability and reliability. These findings highlight the potential of the proposed converter for modern renewable energy applications like solar-powered charging systems, smart DC microgrids, and portable battery devices - especially where space, efficiency, and performance are key considerations.

References

[1] Mojtaba Forouzesh et al., "Step-Up DC-DC Converters: A Comprehensive Review of Voltage-Boosting Techniques, Topologies, and Applications," *IEEE Transactions on Power Electronics*, vol. 32, no. 12, pp. 9143-9178, 2017. [CrossRef] [Google Scholar] [Publisher Link]

[2] Mojtaba Forouzesh et al., "A Survey on Voltage Boosting Techniques for Step-Up DC-DC Converters," *2016 IEEE Energy Conversion Congress and Exposition (ECCE)*, Milwaukee, WI, USA, pp. 1-8, 2016. [CrossRef] [Google Scholar] [Publisher Link]

[3] Abdelfatah Kolli et al., "A Review on DC/DC Converter Architectures for Power Fuel Cell Applications," *Energy Conversion and Management*, vol. 105, pp. 716-730, 2015. [CrossRef] [Google Scholar] [Publisher Link]

[4] Balaji Chandrasekar et al., "Non-Isolated High-Gain Triple Port DC-DC Buck-Boost Converter with Positive Output Voltage for Photovoltaic Applications," *IEEE Access*, vol. 8, pp.113649-113666, 2020. [CrossRef] [Google Scholar] [Publisher Link]

[5] Fabio Corti et al., "Computationally Efficient modeling of DC-DC Converters for PV Application," *Energies*, vol. 13, no. 19, pp. 1-18, 2020. [CrossRef] [Google Scholar] [Publisher Link]

[6] Rajesh Babu Kalahasthi et al., "A Single-Switch High-Gain DC-DC Converter for Photovoltaic Applications," *International Journal of Circuit Theory and Applications*, vol. 50, no. 4, pp.1194-1215, 2022. [CrossRef] [Google Scholar] [Publisher Link]

[7] Keyvan Yari et al., "A New Coupled-Inductor-Based Buck-Boost DC-DC Converter for PV Applications," *IEEE Transactions on Power Electronics*, vol. 37, no. 1, pp. 687-699, 2021. [CrossRef] [Google Scholar] [Publisher Link]

[8] Ramin Rahimi et al., "Z-Source-Based High Step-Up DC-DC Converters for Photovoltaic Applications," *IEEE Journal of Emerging and Selected Topics in Power Electronics*, vol. 10, no. 4, pp. 4783-4796, 2021. [CrossRef] [Google Scholar] [Publisher Link]

[9] Mohammed Alsolami, "A Multi-Input, Multi-Stage Step-Up DC-DC Converter for PV Applications," *Alexandria Engineering Journal*, vol. 60, no. 2, pp. 2315-2324, 2021. [CrossRef] [Google Scholar] [Publisher Link]

[10] Salvador P. Litrán et al., "Single-Switch Bipolar Output DC-DC Converter for Photovoltaic Applications," *Electronics*, vol. 9, no. 7, pp. 1-14, 2020. [CrossRef] [Google Scholar] [Publisher Link]

[11] Julio López Seguel, Jr Seleme I. Seleme, and Lenin M. F. Morais, "Comparative Study of Buck-Boost, SEPIC, Cuk and Zeta DC-DC Converters Using Different MPPT Methods for Photovoltaic Applications," *Energies*, vol. 15, no. 21, pp. 1-26, 2022. [CrossRef] [Google Scholar] [Publisher Link]

[12] Jitendra Bikaneria, Surya Prakash Joshi, and A.R. Joshi, "Modeling and Simulation of PV Cell Using One-diode Model," *International Journal of Scientific and Research Publications*, vol. 3, no, 10, pp. 1-4, 2013. [Google Scholar] [Publisher Link]

[13] Mostafa Karimi Hajiabadi et al., "Non-Isolated High Step-Up DC/DC Converter for Low-Voltage Distributed Power Systems Based on the Quadratic Boost Converter," *International Journal of Circuit Theory and Applications*, vol. 50, no. 6, pp. 1946-1964, 2022. [CrossRef] [Google Scholar] [Publisher Link]

[14] Mahajan Sagar Bhaskar et al., "Modified Multilevel Buck-Boost Converter with Equal Voltage Acrosseach Capacitor: Analysis and Experimental Investigations," *IET Power Electronics*, vol. 12, no. 13, pp. 3318-3330, 2019. [CrossRef] [Google Scholar] [Publisher Link]

[15] Titus Sigamani, Ram Prakash Ponraj, and Vijay Ravindran, "Modified Single Phase Matrix Converter with Z-Source for Renewable Energy Systems," *2020 Third International Conference on Smart Systems and Inventive Technology (ICSSIT)*, Tirunelveli, India, pp. 601-607. 2020. [CrossRef] [Google Scholar] [Publisher Link]

[16] Ram Prakash Ponraj, Titus Sigamani, and Vijay Ravindran, "Analysis of Multi-Input Multilevel Boost Inverter Circuit with Optimal Firing Angles Using dSPACE," *Journal of Electrical Engineering & Technology*, vol. 18, no. 2, pp. 1135-1145, 2023. [CrossRef] [Google Scholar] [Publisher Link]

[17] J.S. Nancy Mary, and K. Mala, "Optimized PV Fed Zeta Converter Integrated with MPPT Algorithm for Islanding Mode Operation," *Electric Power Components and Systems*, vol. 51, no. 13, pp. 1240-1250, 2023. [CrossRef] [Google Scholar] [Publisher Link]

[18] Jeba Singh Oliver et al., "Analysis of Grid-Interactive PV-Fed BLDC Pump Using Optimized MPPT in DC-DC Converters," *Sustainability*, vol. 14, no. 12, pp. 1-14, 2022. [CrossRef] [Google Scholar] [Publisher Link]

[19] Yun Zhang, Jian-Tao Sun, and Yi-Feng Wang, "Hybrid Boost Three-Level DC-DC Converter with High Voltage Gain for Photovoltaic Generation Systems," *IEEE Transactions on Power Electronics*, vol. 28, no. 8, pp. 3659-3664, 2012. [CrossRef] [Google Scholar] [Publisher Link]

[20] Vijayalakshmi Subramanian et al., "A Novel Multilevel DC-DC Flyback Converter Fed H Bridge Inverter," *Journal of Circuits, Systems and Computers*, vol. 32, no. 12, 2023. [CrossRef] [Google Scholar] [Publisher Link]

[21] Zheng Wang et al., "Design and Analysis of a CHB Converter Based PV-Battery Hybrid System for Better Electromagnetic Compatibility," *IEEE Transactions on Magnetics*, vol. 48, no. 11, pp. 4530-4533, 2012. [CrossRef] [Google Scholar] [Publisher Link]

[22] Marikkannu Marimuthu, and Subramanian Vijayalakshm, "Symmetric Multi-Level Boost Inverter with Single Dc Source Using Reduced Number of Switches," *Technical Bulletin*, vol. 27, no. 5, pp. 1585-1591, 2020. [CrossRef] [Google Scholar] [Publisher Link]

[23] Vijay Ravindran et al., "Dynamic Performance Enhancement of Modified SEPIC Converter," *2021 2nd International Conference for Emerging Technology (INCET)*, Belagavi, India, pp. 1-5, 2021. [CrossRef] [Google Scholar] [Publisher Link]

[24] Ahmed Ibrahim Elsanabary et al., "Medium Voltage Large-Scale Grid-Connected Photovoltaic Systems Using Cascaded H-Bridge and Modular Multilevel Converters: A Review," *IEEE Access*, vol. 8, pp. 223686-223699, 2020. [CrossRef] [Google Scholar] [Publisher Link]

[25] Mohammed A. Elgendy, Bashar Zahawi, and David J. Atkinson, "Assessment of the Incremental Conductance Maximum Power Point Tracking Algorithm," *IEEE Transactions on Sustainable Energy*, vol. 4, no. 1, pp. 108-117, 2013. [CrossRef] [Google Scholar] [Publisher Link]